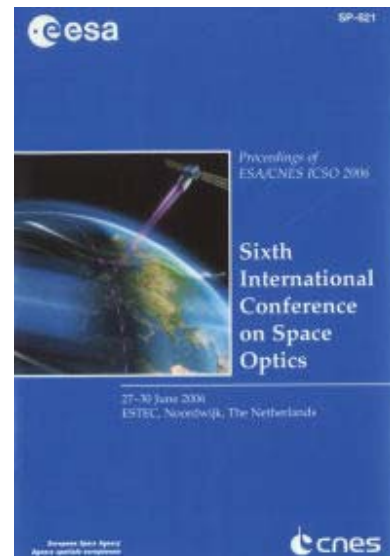


International Conference on Space Optics—ICSO 2006

Noordwijk, Netherlands

27–30 June 2006

Edited by Errico Armandillo, Josiane Costeraste, and Nikos Karafolas



Surface detection performance evaluation of pseudo-random noise continuous wave laser radar

Valentin Mitev, Renaud Matthey, Joao Pereira do Carmo



SURFACE DETECTION PERFORMANCE EVALUATION OF PSEUDO-RANDOM NOISE CONTINUOUS WAVE LASER RADAR

Valentin Mitev⁽¹⁾, Renaud Matthey⁽¹⁾, João Pereira do Carmo⁽²⁾

⁽¹⁾ Observatory of Neuchâtel, rue de l'Observatoire 58, CH2000 Neuchâtel, Switzerland, Email: valentin.mitev@ne.ch

⁽²⁾ ESA- ESTEC, Keplerlaan 1, 2200 AG Noordwijk, The Netherlands, Email: Joao.Pereira.Do.Carmo@esa.int

ABSTRACT

A number of space missions (including in the ESA Exploration Programme) foreseen a use of laser radar sensor (or lidar) for determination of range between spacecrafts or between spacecraft and ground surface (altimetry). Such sensors need to be compact, robust and power efficient, at the same time with high detection performance. These requirements can be achieved with a Pseudo-Random Noise continuous wave lidar (PRN cw lidar). Previous studies have pointed to the advantages of this lidar with respect to space missions, but they also identified its limitations in high optical background.

The progress of the lasers and the detectors in the near IR spectral range requires a re-evaluation of the PRN cw lidar potential. Here we address the performances of this lidar for surface detection (altimetry) in planetary missions. The evaluation is based on the following system configuration: (i) A cw fiber amplifier as lidar transmitter. The seeding laser exhibits a single-frequency spectral line, with subsequent amplitude modulation. The fiber amplifier allows high output power level, keeping the spectral characteristics and the modulation of the seeding light input. (ii) An avalanche photodiode in photon counting detection; (iii) Measurement scenarios representative for Earth, Mercury and Mars.

1. INTRODUCTION

The PRN cw (Pseudo-random noise continuous wave) backscatter laser radar (lidar) with amplitude modulation of the transmitted radiation is described in [1-3] and has been suggested for a number of applications [3-6]. This lidar technique allows the use as transmitter of all solid state sources as laser diodes, fiber amplifiers, etc. The potential result is a compact, robust and power efficient laser radar system, convenient for space missions.

The detection performances of the PRN cw lidar is prone to the optical background more than the ones of the pulse lidar. The performances are also degrade by

stronger scattering features in the probed path [7, 8]. In this respect, the rangefinding and the altimetry are well suited for PRN cw lidar application, because the surface backscatter is much stronger than the scattering originating from subvisible atmospheric features.

The recent progress in the fiber amplifiers, combined with stable single-frequency diode lasers as master oscillators (MO), provides a convenient lidar transmitter for PRN cw lidar. Such transmitter allows the use of ultra-narrow band optical filters what leads to a substantial decrease of the detected optical background. This recent technology development requires a re-considering of the PRN cw lidar applications, already noted in [6]. This study presents performance simulations of surface detection by a perspective PRN cw backscatter lidar on orbiting platform. The considered measurement scenarios are surface probing of the Earth, Mars and Mercury.

2. PRN-CW LIDAR PRINCIPLES

In the PRN cw lidar the probing radiation is modulated by a PRN digital code, where "0"-s and "1"-s correspond to "full power" and "no power" in the transmitted beam [1,2,7]. The cross-correlation function of the detected backscattered signal with the initial PRN code gives the response function of the probed media or respectively, of the probed surface.

The evaluation of the detection performances of the planetary altimeter includes the following: the evaluation of the Signal-to-Noise Ratio for the determination of the peak of the cross-correlation function of the backscattered (back-reflected) signal from the surface. Related to this is the determination of the probability of detection [9] and the range uncertainty [10].

In terms of received number of photons from the surface and from the atmosphere, the SNR of the PRN cw backscatter lidar is expressed as [1-3, 7]

$$SNR(j) = \sqrt{L} \frac{\bar{n}_{s,cc}(j)}{\sqrt{N(\bar{n}_s + \bar{n}_b + \bar{n}_d)}}, \quad (1)$$

The value $\bar{n}_{s,cc}(j)$ is the cross-correlated backscattered photon-counts number arriving from the surface located at altitude range-gate "j", averaged over the sequences. Following [1, 2], this value is given as

$$\bar{n}_{s,cc}(j) = \frac{N+1}{2} \xi_d \tau_c P_0 \bar{g}(j) \quad (2)$$

Here ξ_d is the detection efficiency, P_0 is the averaged transmitted power, τ_c is the single bin duration in the PRN sequence and $\bar{g}(j)$ is the response function of the surface.

In (1) \bar{n}_s , \bar{n}_b and \bar{n}_d are as follows: the mean value of the detected backscattered photon-counts per bin and sequence from all probed ranges (all range gates), the same mean values for the photon-counts of the optical background and the detector dark noise. The values L and N are the numbers of the PRN sequences in the single measurement and the number of the bins in the PRN sequence.

The value \bar{n}_s in the denominator of (1) includes the backscatter signal arriving not only from the surface but also from the atmosphere. In this way, the backscatter and extinction of the atmosphere (determined by its molecular and aerosol components) contributes to the performances of the PRN lidar in two ways: first - by the round-trip attenuation and second - by adding shot-noise via the integrated backscatter signal along the probed profile. In conditions of transparent atmosphere (i.e., no opaque clouds) the atmospheric contribution in this noise term may be small compared to the contribution of the surface backscatter.

3. INPUTS FOR THE NUMERICAL SIMULATIONS

The presented simulations are performed for the concept for a PRN cw lidar altimeter presented in Fig. 1. The transmitter is based on a low-power cw diode laser (further referred as master oscillator or MO). The beam from the MO is modulated by a fast PRN code via convenient optical modulator. The PRN modulated beam is sent to the input of a fiber amplifier. In this way the transmitted beam has the spectral characteristics of the cw laser and the power is determined by the fiber amplifier gain. The bandwidth may be down to hundreds of MHz while the power may exceed several tens of W [11, 12]. The narrow-band transmitter radiation provides the possibility to use in the receiver an ultra-narrow-band filter, a

technique already in development for other space programs [13]. A recent reference for photon counting solid-state detectors is [14]. The basic subsystem specifications of the assumed PRN cw lidar, considered further in the numerical simulations, are presented in Table 1.

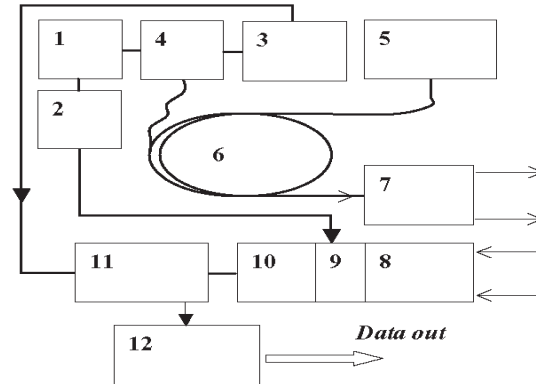


Fig. 1. Conceptual Block-diagram of the PRN cw laser radar (lidar). Legend: 1. MO. 2. Locking chain. 3. PRN code generator and master clock. 4. Optical modulator. 5. High-power pumping laser diodes. 6. Fiber amplifier. 7. Beam shaping and Transmitter optics. 8. Receiver optics. 9. Optical filter. 10. Detector. 11. Signal acquisition. 12. CPU.

Table 1. Subsystem specifications PRN lidar altimeter.

Probing wavelength	1064nm
FWHM of the probing radiation	10pm
PRN code bin duration	1ns
PRN code bin number	$2^{13}-1$
Transmitted mean power, range	5W - 60W
Receiver aperture, Earth	100cm
Receiver aperture, Mars and Mercury	50cm
Receiver field of view	0.02mrad
Optical Filter, FWHM	25pm
Optical Filter transmission	30%
Optical efficiency without the filter	50%
Detector quantum efficiency/dark noise	5% /500sec ⁻¹
Integration time/horizontal resolution	4.096ms/32.7m

We consider the following measurement scenarios: satellite-borne laser radar for altimetry of Earth, Mercury and Mars, where all three cases are considered both in day and night conditions. The influence of the planetary atmosphere (critical both in attenuator and backscattering) is accounted in the cases of Earth and Mars probing. The relevant parameters for the numerical simulations are presented in Table 2.

The objective of this work is only a feasibility study of the PRN cw lidar performance with respect to altimetry, so the selected subsystem performances may

be characterised only as "representative", taking into account the present day optical technology. There is no attempt in the presented work for optimisation of subsystem specifications or definition of requirements.

Table 2. Characteristics of the considered measurement scenarios.

Lidar (satellite) altitude,	Earth and Mercury: 800km; Mars: 450km;
Probing direction	Nadir
Molecular atmosphere, Earth	US standard atmosphere, 1976
Aerosol components, Earth and Mars	Single layer between 2-2.6km above surface;
Aerosol optical depth	0, 0.2, 0.3; all at 532nm
Optical background, daytime Earth	~0.52W/m ² nm, as in [6]
Optical background, day time Mercury and Mars	calculated from [6], with respect to the average distance from the Sun
Sun zenith angle, all	45°
Optical background, nighttime, all	~the daytime value, multiplied by a factor 10 ⁻⁵
Surface	Lambertian; Normal to the probing direction,
Surface albedo	0.3

The consistency of this approach was tested using a PRN cw lidar demonstrator described in [15].

The demonstrator operates with a cw laser diode at 780nm with a transmitted power of 11mW and a photon-counting detector. The diameter of the receiver telescope is 20cm. The PRN bin and sequence length were respectively 100ns and 9 bit.

Fig. 2 presents the cross-correlated signal from a masonry surface located at 4400m from the lidar with integration time of 0.204sec. This measured signal is compared with a calculated one. To define the inputs for this signal calculations, the lidar specifications and the albedo of the probed surface were carefully evaluated in series of calibration measurements. The specifications were used as inputs in the numerical simulations of a signal from the masonry wall, with realistic assumptions for the atmospheric contribution in round-trip transmission and the atmospheric backscatter.

The result from the calculations of the PRN cw cross-correlated signal is presented in Fig. 3. As we may see, the result from the simulations appears almost identical to the measurement, what gives a confidence to the approach used in this work.

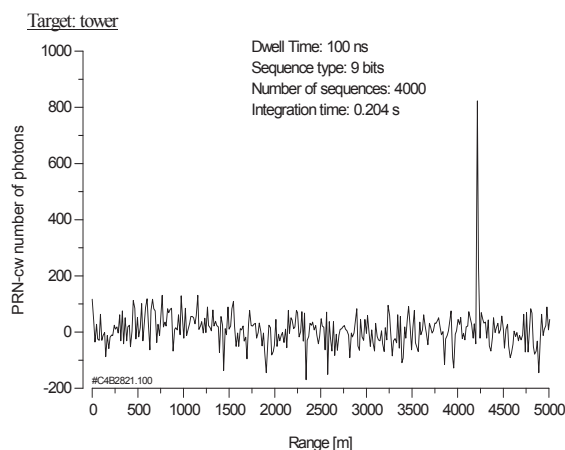


Fig.2. Cross-correlated backscatter signal from a wall: measured with a PRNcw lidar demonstrator.

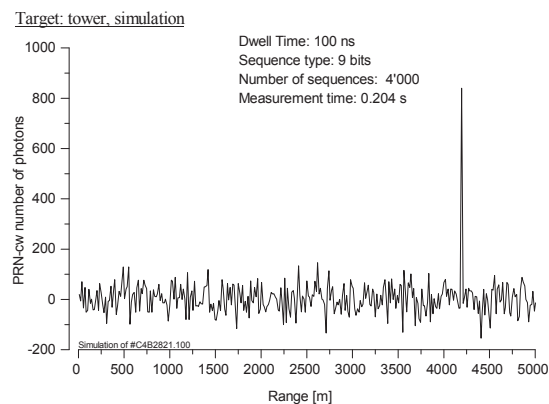


Fig.3. Calculated cross-correlated backscatter signal from a wall for the measurement case in Fig. 2.

4. NUMERICAL RESULTS: PROBING OF EARTH SURFACE

Fig. 4 presents the calculated PRN cw cross-correlated lidar signal in the following scenario: probing Earth surface, night-time, surface at 500m asl (above sea level).

The determination of the range (altitude) to the surface from the cross-correlated PRN cw lidar response may follow the "threshold approach", similar as it is in the pulse laser altimeters [16]. In evaluation of the detection performances of the planetary altimeter in such approach it is of importance to calculate also the cumulative probability for surface detection. In the case of the PRN cw lidar this value is the cumulative probability to obtain cross-correlated signal above a given threshold. Since in the considered case the detection is in photon-counting mode the probability shall be calculated for Poisson signal statistics [6].

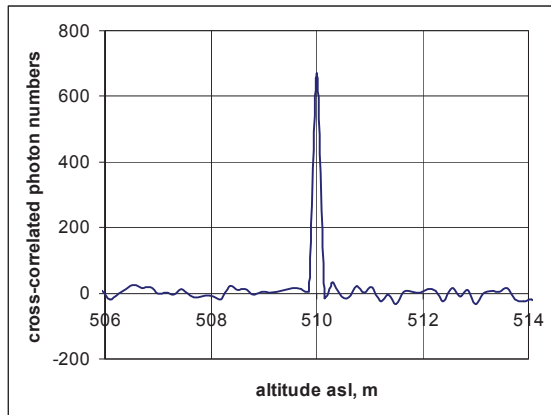


Fig. 4. The calculated cross-correlated PRN cw lidar signal from Earth surface at 500m asl, daytime.

Both the probability of detection and the range uncertainty are functions of the SNR, i.e., the starting "figure of merit" in such evaluation is the calculation of the SNR.

Fig. 5 presents representative examples for the SNR of surface detection. The results from the calculations are presented for both nighttime and daytime. The detection probability and the range (altitude) uncertainty are presented only for daytime case in Figs. 6 and 7.

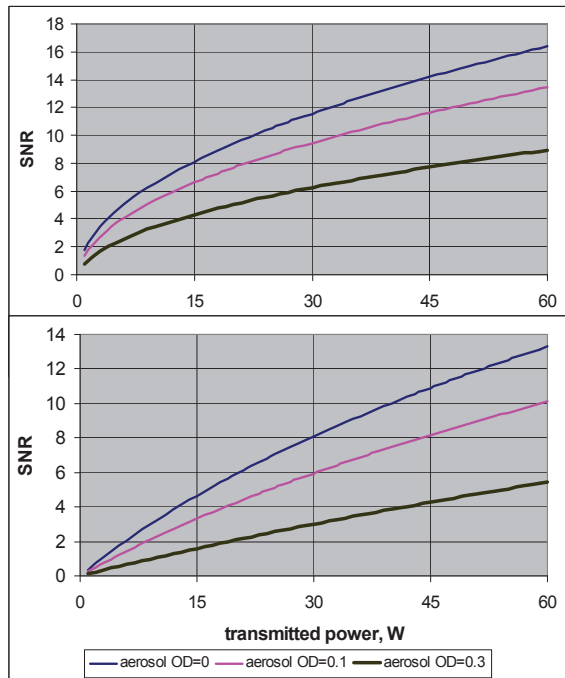


Fig. 5. The SNR for surface signal detection with PRN cw lidar altimeter; Earth; Subsystem specifications are as in Table 1, scenario parameters as in Table 2. Upper panel: night time; Lower panel: daytime.

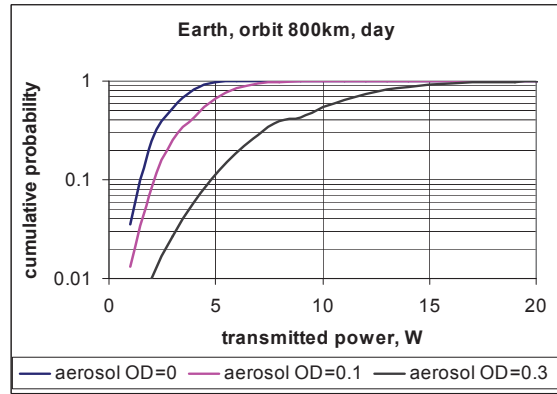


Fig. 6. Cumulative probability of detection for Earth probing, for three values of the atmospheric aerosol OD; daytime.

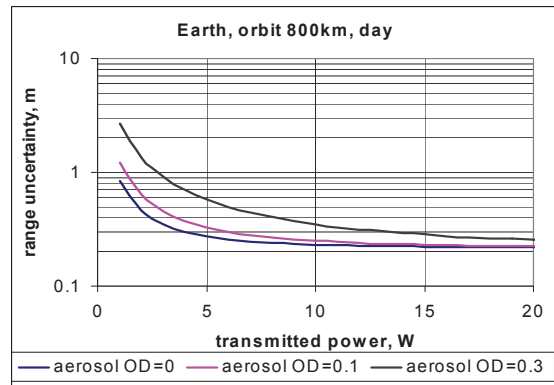


Fig. 7. Range (altitude) uncertainty for Earth probing PRN cw lidar altimeter for three values of the atmospheric aerosol OD; Daytime.

The results in Figs. 6 and 7 show that a detection probability of more than 98% may be achieved for transmitted power of 20-30W. The ranging error may reach 23 -25cm, where the PRN clock bin is 1ns. It shall be noted that the SNR depends on the integration time of the measurement, not on the duration of the clock bin. That is, with a shorter bin of the PRN modulation code, the ranging error may be decreased with respect to the one in Fig. 7, with the same integration time.

5. NUMERICAL RESULTS: PROBING MARS AND MERCURY SURFACE

From point of view of PRN cw lidar, the probing of Mars and Mercury surfaces, shall account for different problems. Mars is a planet with atmosphere containing a aerosol, determining considerable optical depth [17,

18]. Mercury does not present such problem. On the other hand, the daytime optical background at Mercury orbit is about 16 times higher than the one at Mars orbit, what creates stronger requirements for the bandwidths of the transmitted beam and the optical filter.

In this sense, it is interesting to see how the detection performances will differ for daytime and nighttime probing for these two planets. Here we present only the detection probably and range uncertainty.

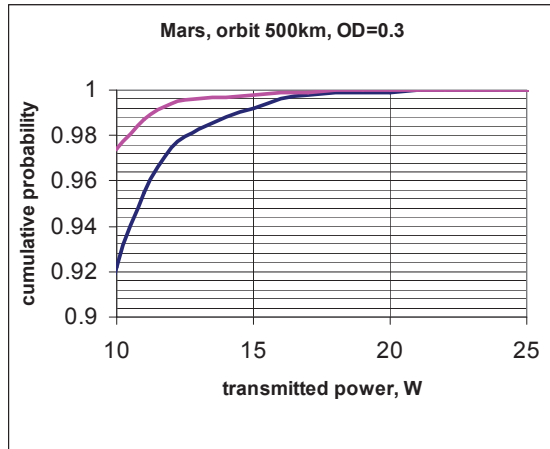


Fig. 8. Cumulative probability of detection for Mars surface; aerosol OD=0.3; nighttime (red line) and daytime (blue line).

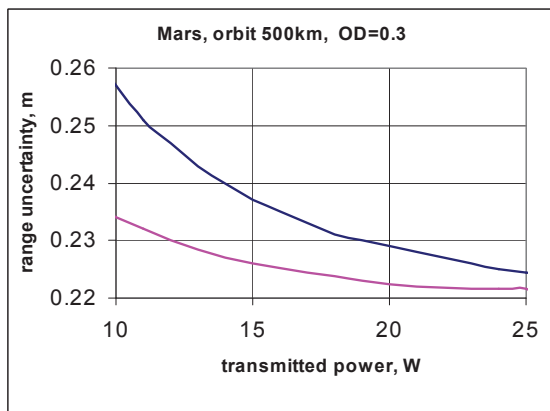


Fig. 9. Range (altitude) uncertainty, Mars surface; aerosol OD=0.3; nighttime (red line) and daytime (blue line).

The results for Mars are presented in Figs. 8 and 9. The results for Mercury are presented in Fig. 10 and 11. The presented results in Figs. 8 and 9 demonstrate that the PRN cw altimeter may be very convenient for Mars

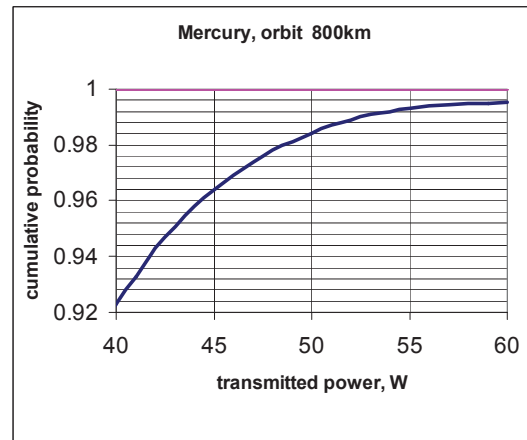


Fig. 10. Cumulative probability of detection for Mercury surface; nighttime (red line) and daytime (blue line).

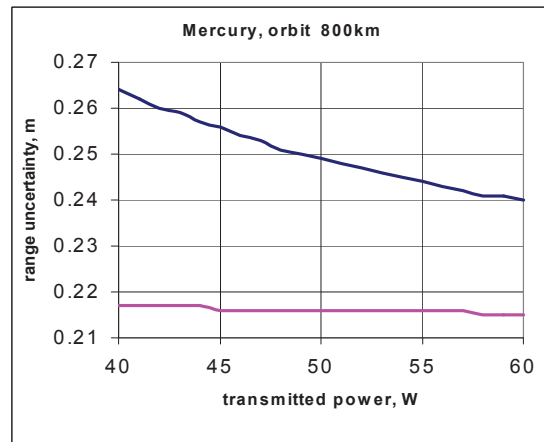


Fig. 11. Range (altitude) uncertainty, Mercury surface; nighttime (red line) and daytime (blue line).

(as well as for planets and moons beyond the orbit of Mars). High detection probability and low range uncertainty are achieved with a moderate transmitted power of 15-20W, even for a considerable aerosol OD. It shall be noted that this performances are for a lidar with receiver diameter of 50cm, i.e. the same as in the already operational altimeter MOLA [16] and much less than the one assumed for Earth probing (Table 1).

The results for Mercury probing are different. As it may be expected, the performances in the nighttime probing are relatively high. On the other hand, due to the high level of the optical background, to obtain reasonable performances during the daytime probing a transmitter power of more than 40W is required.

5. CONCLUSION

From the presented results we may conclude the following:

- With the availability of novelty optical technologies (fiber amplifier combined with narrow-band MO, photon-counting detector and narrow-band filters) the PRN cw laser radar demonstrates very good performances for planetary altimetry in a number of representative scenarios.
- Substantial advantage of the PRN cw laser radar as altimeter is that, unlike the pulsed laser radar, there is no missed spots along the track on the surface. It shall be noted that the along-track resolution in the presented evaluation is only 32.7m.
- To the excellent detection performances during both night and daytime, it shall be added the advantaged offered by the potential technologies – compact and robust design, high power efficiency, durability and long life. These features of the potential technology make the PRN cw laser radar a convenient candidate for space missions.

The fiber amplifiers, suggested for use in this concept, are industrial product with applications in the telecommunication and in the material processing. These devices are suited for operation with high duty cycle and are optimal as PRN cw lidar transmitter. The detector technology based on photon counting APD is also industrial product. Narrow-band filters are realised with respect for perspective Space missions.

As it was already pointed, the objective of this study is only a demonstration of the feasibility of the PRN lidar approach to planetary altimetry. Anyway, the present approach and numerical tools may be used in future optimisation of such sensors, with respect to the imposed detection requirements in specific applications.

ACKNOWLEDGMENTS

This work is supported by ESA/ESTEC and by the State of Neuchâtel.

REFERENCES

1. Takeuchi N., et al. "Random modulation cw lidar", Applied Optics, Vol. 22 No. 9, pp. 1382-1386, 1983.
2. Takeuchi N. et al., "Diode-laser random-modulation cw lidar", Applied Optics., Vol. 25, pp. 63-67, 1986.
3. Abshire J.B., et al, "Altimetry and lidar using AlGaAs laser modulated with pseudo-random codes", 16th ILRC, Nasa Conference Publication, Vol. 3158, part 2, p.441-445, Boston, 1992.
4. Nasagava C. et al, "Random modulation CW lidar using a new random sequence", Applied Optics, Vol. 29, 1466-1470, 1990.
5. Norman D.M, Gardner C.S., "Satellite laser ranging using pseudonoise code modulated laser diodes", Applied Optics, Vol. 27, 3650, 1988.
6. Abshire J. B. et al, "Laser Altimetry Using Pseudo Noise Code Modulated Fiber Lasers and Photon Counting Detectors", CLEO/QELS and PhAST, May 22-27, 2005, Baltimore – USA. Paper JTh14.
7. Matthey R, Mitev V., "Computer model study of pseudo-random noise modulation, continuous-wave (PRN-cw) backscatter lidar", SPIE Volume 2505, 140-149, 1995.
8. Machol Janet L., "Comparison of the pseudorandom noise code and pulsed direct-detection lidars for atmospheric probing" Appl. Optics, Vol. 36, No. 24, p.p., 6021-6023, 1997.
9. Jelalian A.V., "Laser Radar Systems", Artech House, London-Boston, 1991.
10. Carmer D. C. and Peterson L. M., "Lares radar in robotics", Proc. IEEE, vol. 84, 299-320, 1996.
11. Yusim A. et al., "100 watt single –mode CW lineary polarised all-fiber format 1.56 μ m laser with suppression of parasitic lasing effects", in Fiber Lasers II: Technology, Systems and Applications, 24-27 January 2005 San Jose-USA. SPIE Volume 5709, 69-77, 2005.
12. Liem A., et al., "100-W single frequency master-oscillator fiber power amplifier", Opt. Lett., Vol. 28, 1537- 1539, 2003.
13. Bond R. A. et al., "High-resolution optical Filtering technology", 22nd ILRC, Matera, Italy, 12-16 July 2004, Proceedings ESA SP-561, 239-242, 2004..
14. Pauchard A., A. Rochas, "Single-Photon Counters get a second wind", Photonic Spectra, March 2005, 102-106.
15. Matthey R. et al, "PRN-cw backscatter measurements with a powerful narrowband diode laser", in Advances of Atmospheric Remote Sensing with Lidar - Selected papers of the 18th ILRC. Springer, 115-118.1997
16. Abshire J.B., Xiaoli Sun and Robert S. Afzal, "Mars Orbiter Laser Altimeter: receiver model and performance analysis", Appl. Opt., Vol. 39, 2449-2460, 2000.
17. Pollack J.B., Ockert-Bell M.E., Shepard M.K., "Viking Lander image analysis of Martian atmospheric dust", J. Geophys. Res., Vol. 100, No. E3, pp. 5235-5250, 1995.
18. Smith P.H., et al, "Results from the Mars Pathfinder camera", Science, No. 278, pp. 1758-1765, 1997.